Mon. Not. R. Astron. Soc. **000**, 000–000 (2010) Printed 10 August 2010 (MN LATEX style file v2.2)

Tides and Tidal Engulfment in Post-Main Sequence Binaries: Period Gaps for Planets and Brown Dwarfs Around White Dwarfs

J. Nordhaus[1⋆], D. S. Spiegel[1,2], L. Ibgui[1,3], J. Goodman[1], A. Burrows[1,2]
[1] *Department of Astrophysical Sciences, Princeton University, Princeton, NJ 08544, U.S.A.*
[2] *Kavli Institute for Theoretical Physics, UCSB, Santa Barbara, CA 93106, U.S.A.*
[3] *LERMA, Observatoire de Paris, CNRS et UPMC, 5 place J. Janssen, 92195 Meudon, France*

arXiv:1002.2216v4 [astro-ph.SR] 9 Aug 2010

Submitted 25 February 2010

ABSTRACT

The presence of a close, low-mass companion is thought to play a substantial and perhaps necessary role in shaping post-Asymptotic Giant Branch and Planetary Nebula outflows. During post-main-sequence evolution, radial expansion of the primary star, accompanied by intense winds, can significantly alter the binary orbit via tidal dissipation and mass loss. To investigate this, we couple stellar evolution models (from the zero-age main-sequence through the end of the post-main sequence) to a tidal evolution code. The binary's fate is determined by the initial masses of the primary and the companion, the initial orbit (taken to be circular), and the Reimers mass-loss parameter. For a range of these parameters, we determine whether the orbit expands due to mass loss or decays due to tidal torques. Where a common envelope (CE) phase ensues, we estimate the final orbital separation based on the energy required to unbind the envelope. These calculations predict period gaps for planetary and brown dwarf companions to white dwarfs. The upper end of the gap is the shortest period at which a CE phase is avoided. The lower end is the longest period at which companions survive their CE phase. For binary systems with 1 $M_\odot$ progenitors, we predict no Jupiter-mass companions with periods $\lesssim$270 days. Once engulfed, Jupiter-mass companions do not survive a CE phase. For binary systems consisting of a 1 $M_\odot$ progenitor with a companion 10 times the mass of Jupiter, we predict a period gap between $\sim$0.1 and $\sim$380 days. These results are consistent with both the detection of a $\sim$50 $M_{\rm J}$ brown dwarf in a $\sim$0.003 AU ($\sim$0.08 day) orbit around the white dwarf WD 0137-349 and the tentative detection of a $\sim$2 $M_{\rm J}$ planet in a $\gtrsim$2.7 AU ($\gtrsim$4 year) orbit around the white dwarf GD66.

Key words: stars: AGB and post-AGB – stars: low-mass, brown dwarfs, planetary nebulae: general

1 INTRODUCTION

For low- and intermediate-mass stars (initially $\lesssim$8 $M_\odot$), post-main sequence (post-MS) evolution is characterized by expansion via giant phases accompanied by the onset of mass-loss. In particular, during the Asymptotic Giant Branch phase (AGB), dust-driven winds expel the stellar envelope as the star begins its transition to a white dwarf (WD). However, before formation of the WD remnant, the spherical outflows observed during the AGB phase undergo a dramatic transition to the highly asymmetric and often bipolar geometries seen in the post-AGB and planetary nebula phases (PN; Sahai and Trauger 1998). This transition is often accompanied by high-speed, collimated outflows. For recent reviews see Balick and Frank (2002), van Winckel (2003), de Marco (2009).

A central hypothesis to explain shaping in post-AGB/PNe is that a close companion is necessary to power and shape bipolarity. This is supported by observations of excess momenta in almost all post-AGB outflows relative to what isotropic radiation pressure can provide (Bujarrabal et al. 2001). Additionally, close companions have been detected in or around giants, bipolar post-AGB and PNe systems and in some cases seem to be responsible for outflow shaping (Silvotti et al. 2007; De Marco et al. 2008; Sato et al. 2008b,a; Witt et al. 2009; Miszalski et al. 2009b,a;

⋆ E-mail: nordhaus@astro.princeton.edu

© 2010 RAS

Niedzielski et al. 2009; Chesneau et al. 2009). In particular, the recent detection of a white dwarf with an orbiting $\sim$50 $M_{\rm J}$ brown dwarf in a $\sim$2 hour orbit demonstrates that low-mass companions can survive a common envelope phase (CEP) (Maxted et al. 2006). The detection of a planetary companion ($M\sin i = 3.2$ $M_{\rm J}$) around the extreme horizontal branch star V391 Pegasi in a $\sim$1.7 AU orbit ($\sim$3.2 year period; Silvotti et al. 2007) and the tentative detection of a $\sim$2 $M_{\rm J}$ planet in a $\gtrsim$2.7 AU orbit ($\gtrsim$4 year period; Mullally et al. 2008, 2009) around the white dwarf GD66 provide motivation for this work.

Indirect observational evidence for binarity comes from maser observations that suggest magnetic jet collimation in AGB and young post-AGB stars (Vlemmings et al. 2006; Sabin et al. 2007; Vlemmings and van Langevelde 2008). Such collimation supports the binary hypothesis because it is difficult for single AGB stars to generate the large field strengths necessary to power the outflows without an additional source of angular momentum (Nordhaus et al. 2007, 2008a). If a close companion is present, strong interactions can transfer energy and angular momentum from the companion to the primary. In particular, if the companion is engulfed in a common envelope (CE), rapid in-spiral can cause significant differential rotation of the envelope (Nordhaus and Blackman 2006; Nordhaus et al. 2008b). Coupled with a strong convective envelope, large-scale magnetic fields are amplified and are sufficient to unbind the envelope and power the outflow (Nordhaus et al. 2007).

Moe and De Marco (2006) overpredicted the Galactic PN population by a factor of $\sim$6 for PN with radii $\lesssim$0.9 pc (discrepant at the 3 σ level; Jacoby 1980; Peimbert 1990). This discrepancy could be alleviated if only a fraction of stars become PNe. The authors argue that perhaps interacting binaries or, in particular, common envelope systems may be responsible for producing the majority of Galactic PNe (De Marco and Moe 2005). However, to determine the validity of a hypothetical CE/PN connection, it is important to understand which binary systems will undergo a CE phase during their evolution. The fact that low-mass stellar companions can survive CE evolution motivates further study independent of a potential connection to PNe (Maxted et al. 2006).

Various aspects of tides on the evolution of post-MS binaries have previously been investigated (Rasio et al. 1996; Carlberg et al. 2009; Villaver and Livio 2009). Recently, Carlberg et al. (2009) aimed to understand fast rotation in field RGB stars, while Villaver and Livio (2009) focused on trying to predict the distribution of planets around evolved stars. Carlberg et al. (2009) calculated orbital evolution scenarios but neglected mass-loss effects. Villaver and Livio (2009) included stellar mass-loss in their model and modeled a range of progenitor masses (from 1 to 5 $M_{\odot}$), but did not examine how results depend on the prescriptions for either tidal interactions or stellar mass loss. They considered a wide range of possible astrophysical effects, including frictional and gravitational drag, wind accretion, and atmospheric evaporation. We neglect these effects in our study; most are negligible compared to tidal torques and mass loss from the primary. The exception is perhaps evaporation, which has been claimed to destroy planets of mass $< 15 M_{\rm J}$ (Villaver and Livio 2007; Livio and Soker 1984). This is similar to the minimum mass required to unbind the stellar envelope (Section 6). Our work builds upon both previous results in that we follow the evolution from the zero-age main sequence (ZAMS) through the entire post-MS, and we consider a variety of prescriptions for tidal torque and for stellar mass-loss rates.

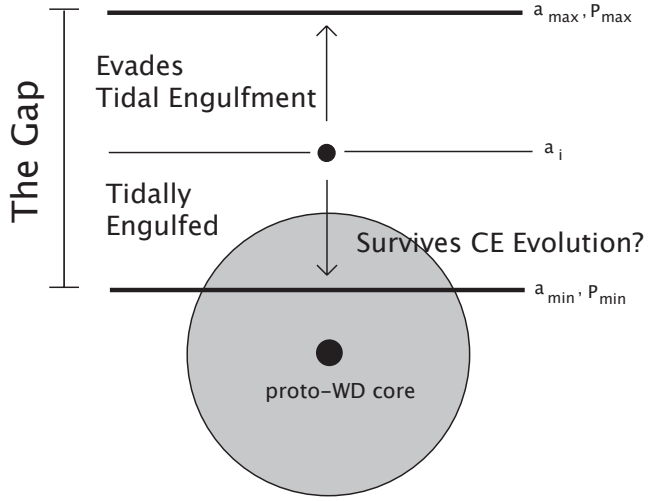

Figure 1. The period gap for low-mass companions around white dwarfs. The orbit of a companion located initially at a_i decays and plunges into the giant star. Depending on the mass of the companion and stellar structure at plunge time, the companion may or may not survive the CE phase. Companions slightly exterior to a_i avoid engulfment and never enter a CE; their orbits expand due to mass-loss. The gap is set by the final maximum semimajor axis which survives CE evolution ($a_{\rm min}$) and the final minimum semimajor axis which avoids tidal engulfment ($a_{\rm max}$).

In this paper, we investigate how low-mass companions ($\lesssim$0.1 $M_{\odot}$) become immersed in a common envelope. By coupling stellar evolution models to tidal evolution equations, we can determine when (i) mass-loss dominates and leads to orbital expansion or (ii) dissipation of tidal energy dominates and leads to orbital reduction. In particular, for a given orbital separation, we can determine which binary systems incur a CE by plunging into their host stars modulo the uncertainties in the theories of tidal dissipation and stellar mass-loss. In §2, we describe our equations and discuss a possible tidal dependence on period. In §3, we present our stellar evolution models and focus on low-mass companions (planets, brown dwarfs and low-mass main sequence stars). In §4, we present our results and discuss the implications of two commonly used tidal prescriptions. For systems that incur a CE, we use an energetics argument to determine the maximum radius at which a given companion can survive the interaction by successfully ejecting the envelope. Furthermore, we determine the minimum separation that evades a CE phase. By explicitly following the orbital evolution, we calculate the final separation of the binary system. For a given binary, this produces a gap inside of which we expect the absence of companions. From the set of all gaps, we can determine a minimum period gap for planetary companions around white dwarfs (see Fig. 1). The prediction of a gap should be of interest to recent searches for both substellar and, in particular, planetary companions to white dwarfs in addition to future observations (Mullally et al. 2008, 2009; Kilic et al. 2010; Qian et al. 2010). We discuss these results

in §5 and §6. In §7, we discuss the possibility of detecting WD+companion transits and applications to *GALEX* data. We conclude in §8.

2 TWO-BODY TIDES

We employ a two-body gravitational and tidal interaction model that consistently couples the evolution of the mass and the radius of the primary star with the orbit of the companion. It includes the tides raised on the companion (by the star) and the tides raised on the star (by the companion).

The evolution of the semimajor axis (a) is due to two contributions: the tidal interaction between the primary and the companion and the mass loss of the primary

$$\frac{da}{dt} = \left(\frac{da}{dt}\right)_{\rm tides} + \left(\frac{da}{dt}\right)_{\rm mass\ loss} . \quad (1)$$

We employ the equations of Ferraz-Mello et al. (2008), which use the Q-formalism of Goldreich (1963) for the tidal evolution of the orbital eccentricity, e and the semimajor axis, a. This approach has been used extensively to model the inflated radii and orbits of transiting extra-solar giant planets (EGP; Kaula 1968; Ferraz-Mello et al. 2008; Jackson et al. 2008; Ibgui and Burrows 2009; Miller et al. 2009; Ibgui et al. 2009; Jackson et al. 2009).

Our formalism assumes that the primary star and companion are both spherical and that their rotational and orbital angular momenta are aligned. Furthermore, we assume the companion spin is synchronized with its orbital period and that the mean orbital motion is greater than the stellar rotation rate. This is reasonable as typical equatorial surface velocities are $\sim 1-3$ km s^{-1} for low-mass giants implying that, for companions that are close enough for tides to matter in the post-main-sequence evolution, the angular velocity of the orbit is much greater than the angular velocity of the primary star (Gray 1989; Massarotti et al. 2008). Under these assumptions, we have that

$$\frac{1}{a}\frac{da}{dt} = -\frac{1}{a^{13/2}}\left[2K_1\frac{R_c^5}{Q_c'}e^2 + \frac{8}{25}\left(1+\frac{57}{4}e^2\right)K_2\frac{R_\star^5}{Q_\star'}\right]$$
$$\frac{1}{e}\frac{de}{dt} = -\frac{1}{a^{13/2}}\left[K_1\frac{R_c^5}{Q_c'} + K_2\frac{R_\star^5}{Q_\star'}\right] , \quad (2)$$

where R_c and $R_\star$ are the companion and primary radii, Q_c' and $Q_\star'$ are the tidal dissipation factors of the companion and the primary and $K_{1,2}$ are constants given by

$$K_1 = \frac{63}{4}\left(GM_\star\right)^{1/2}\frac{M_\star}{M_c}$$
$$K_2 = \frac{225}{16}\left(GM_\star\right)^{1/2}\frac{M_c}{M_\star} , \quad (3)$$

where M_c is the companion mass and $M_\star$ is the primary mass.

Furthermore, the radius and mass of the companion are held constant while those of the primary are time-dependent. Note that in these equations, e can only decrease and if the primary mass were constant, a could only decrease as well.

The tidal dissipation factors Q_c' and $Q_\star'$ are dimensionless parameters given by $Q' = 3Q/2k_2$, where Q is the specific tidal dissipation function and k_2 is the Love number (Goldreich 1963; Goldreich and Soter 1966; Ogilvie and Lin 2007). Q is a dimensionless parameter that quantifies the efficiency of tidal dissipation inside a body. It is defined by its reciprocal, the specific dissipation function

$$Q^{-1} = \frac{1}{2\pi E_0}\oint\left(-\frac{dE}{dt}\right)dt , \quad (4)$$

where E_0 is the maximum energy stored in the tidal distortion of the body and the integral $\oint\left(-\frac{dE}{dt}\right)dt$ is the energy dissipated over one orbital cycle (Goldreich 1963). Typical estimates yield $Q_\star' \sim 10^{5.0-8.0}$, $Q_c' \sim 10^{5.5-6.5}$ for Jupiter mass planets around main-sequence stars and $Q'_{\rm Jupiter} \sim 10^{5.5-6.0}$ (Goldreich and Soter 1966; Yoder and Peale 1981; Ogilvie and Lin 2004, 2007; Jackson et al. 2009)

2.1 Primary and Companion Tides

Tides on the primary act to synchronize its spin while tides on the companion act to circularize the orbit. We can compare the tides raised on the companion (induced by the primary) to the tides raised on the primary (induced by the companion) as follows:

$$\frac{(da/dt)_c}{(da/dt)_\star} = \left(\frac{7e^2}{1+\frac{57}{4}e^2}\right)\left(\frac{M_\star}{M_c}\right)^2\left(\frac{Q_\star'}{Q_c'}\right)\left(\frac{R_c}{R_\star}\right)^5 \quad (5)$$
$$\frac{(de/dt)_c}{(de/dt)_\star} = \frac{28}{25}\left(\frac{M_\star}{M_c}\right)^2\left(\frac{Q_\star'}{Q_c'}\right)\left(\frac{R_c}{R_\star}\right)^5 . \quad (6)$$

For a 1 $M_\odot$ AGB star (with radius $\sim$1 AU) and a 0.1 $M_\odot$ main sequence companion (with radius $\sim$0.1 $R_\odot$), with $e = 0.1$, we have

$$\dot{a}_c/\dot{a}_\star \sim 10^{-16}\left(Q_\star'/Q_c'\right) \quad (7)$$
$$\dot{e}_c/\dot{e}_\star \sim 10^{-15}\left(Q_\star'/Q_c'\right) . \quad (8)$$

For lower mass companions, these ratios remain extreme. Therefore, for $Q_\star' \simeq Q_c'$, if the primary is a post-main sequence star, the orbit decays almost entirely due to tides raised on the star, not to those raised on the companion.

As the orbit circularizes ($e \to 0$), the tides on the companion decrease until they vanish for perfectly circular orbits. However, note that some dissipation must occur within the companion to maintain synchronous rotation. In this limit, the orbital evolution is governed by non-synchronous rotation between the companions orbit and spin of the primary. As a result, in-spiral continues and might lead to the companion plunging into the primary (the cases we are interested in here).

2.2 Main-sequence and Post-MS Tides

For the known extrasolar giant planets (EGPs), the tides raised on the primary can be substantial and can lead to significant orbital reduction during the main-sequence (Ibgui and Burrows 2009; Levrard et al. 2009; Ibgui et al. 2009; Spiegel et al. 2010). For the same $Q_\star'$, we can estimate whether a similar reduction is expected during the post-MS. From the previous section, we have that the tides on the primary dominate and, hence,

$$\frac{\Delta \ln a_{\rm rgb}}{\Delta \ln a_{\rm ms}} \sim \left(\frac{R_{\rm rgb}}{R_{\rm ms}}\right)^5\left(\frac{a_{\rm rgb}}{a_{\rm ms}}\right)^{-13/2} \times \left(\frac{M_{\rm c,rgb}}{M_{\rm c,ms}}\right)\left(\frac{\tau_{\rm rgb}}{\tau_{\rm ms}}\right)\left(\frac{Q'_{\star,rgb}}{Q'_{\star,agb}}\right)^{-1} , \quad (9)$$

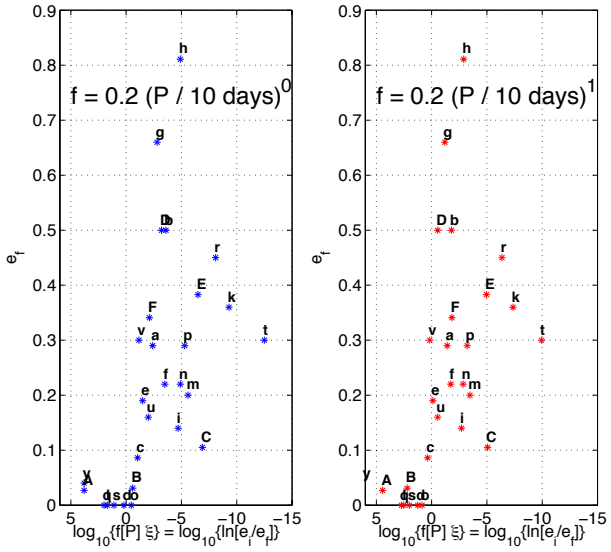

Figure 2. Reproduced versions of Fig. 4c of (Verbunt and Phinney 1995) assuming a period dependence on f. The transition between circularized and non-circularized systems is preserved around unity for a variety of scalings. Here we present one example. Left: $f \propto P^0$ which implies $Q'_\star \propto P$. Right: $f \propto P^1$ which implies $Q'_\star \propto P^0$.

where $\tau_{\rm ms}$ is the typical lifetime during the main sequence and $\tau_{\rm rgb}$ is the lifetime during the RGB phase.

For the main sequence, we take a 1 Jupiter mass companion around a 1 $M_\odot$ main-sequence primary with semi-major axis $\sim$0.05 AU. For the RGB phase, we assume that the companion is orbiting at 1.3 AU, that $Q'_{\star,{\rm ms}} = Q'_{\star,{\rm rgb}}$ and that $R_{\rm rgb} \sim 10^2 R_{\rm ms}$ and $\tau_{\rm rgb} \sim 10^{-2}\tau_{\rm ms}$. Using these parameters yields $\Delta{\rm ln}a_{\rm rgb}/\Delta{\rm ln}a_{\rm ms} \sim 0.063$. Therefore, for this system, we expect tides to be weaker on the RGB phase than they are for EGP systems. This is likely to be true for low-mass primaries ($\lesssim 1.5 M_\odot$) where radial expansion during the RGB is substantial (see Fig. 3). For higher mass primaries, radial expansion is minimal during the RGB and extensive during the AGB. However, typical AGB lifetimes are $\sim 10^{-2}$–$10^{-3}\tau_{\rm rgb}$. We can estimate the effect of tides during the AGB phase in the same way. Assuming $R_{\rm agb} \sim 200$ $R_\odot$, $Q'_{\star,{\rm ms}} = Q'_{\star,{\rm agb}}$ and $\tau_{\rm agb} \sim 10^{-5}\tau_{\rm ms}$, we have that $\Delta{\rm ln}a_{\rm agb}/\Delta{\rm ln}a_{\rm ms} \sim 2.0 \times 10^{-3}$. Thus in general, we expect synchronization tides on the AGB to be weaker both than those on the RGB and for typical EGPs around main sequence stars. Note the steep dependence on the ratio of the stellar radii in Eq. 9. If $R_{\rm agb} = 2R_{\rm rgb}$ and $\tau_{\rm agb} = (1/30)\tau_{\rm rgb}$, then $\Delta{\rm ln}a_{\rm agb}/\Delta{\rm ln}a_{\rm rgb} \sim 1$ and tides are approximately equal during the RGB and AGB phases. However, as will be seen shortly, there is reason to expect that Q'_* may be orders of magnitude smaller on the giant branches than on the main sequence for the same a/R_*, with a corresponding increase in the importance of the advanced evolutionary phases for the orbit.

2.3 A Period Dependence of $Q'_\star$?

It is worth nothing that the work of Goldreich (1963) and Goldreich and Soter (1966) does not specify a tidal dissipation mechanism. Zahn (1966) however, proposed a tidal theory based on turbulent viscosity. This theory was tested and calibrated in stellar binaries that contain an evolved star primary (Verbunt and Phinney 1995). Evolved stars are expected to possess extended convective zones, which could be crucial for tidal dissipation. In their formalism, the authors introduce a dimensionless factor f that is calibrated via the orbital eccentricity measurements in their post-MS binary sample. The authors argue that observational data imply that f is constant and approximately unity.

By setting equal the expression for the tidal torque (as a function of $Q'_\star$) in Goldreich and Soter (1966) to the expression (as a function of f) in Zahn (1989), as simplified by Verbunt and Phinney (1995), we have that

$$\begin{aligned} Q'_\star &= \frac{63}{16\pi}\frac{GM_\star}{R_\star^3}\frac{M_\star}{fM_{\rm env}}\left(\frac{M_{\rm env}R_\star^2}{L}\right)^{1/3} P \qquad (10) \\ &\propto \frac{\tau_{\rm conv}}{\tau_{\rm dyn}^2} P \end{aligned}$$

where $M_{\rm env}$ is the mass of the convective envelope, P is the orbital period, $\tau_{\rm conv}$ is the convective timescale and $\tau_{\rm dyn}$ is the dynamical timescale. If f is in fact constant, then $Q'_\star$ is proportional to orbital period. Note that the numerical prefactor in Eq. (10) ($63/16\pi$) is slightly different from the $225/32\pi$ that results from setting our expresion for $d\ln e/dt$ (in Eq. 2) equal to the corresponding expresion in Verbunt and Phinney (1995). The difference (compared to the variation in period) is sufficiently small that it does not effect our results.

The argument for f constant and $\sim$1 derives from Fig. 4c of Verbunt and Phinney (1995). The transition between circularized and non-circularized systems occurs when the abscissa is 0. The abscissa is given by $\log_{10}\{-\Delta\ln[{\rm e}]/{\rm f}\} = \log_{10}\{\ln[{\rm e_i}/{\rm e_f}]\} - \log_{10}\{{\rm f}\}$. If $\log_{10}\{\ln[{\rm e_i}/{\rm e_f}]\}$ is greater than (less than) 0, the system is strongly (barely) circularized. The transition occurs near $\log_{10}\{\ln[{\rm e_i}/{\rm e_f}]\} = 0$. Looking at Fig. 4c of Verbunt and Phinney (1995), we see this transition happens at $\log_{10}\{\ln[{\rm e_i}/{\rm e_f}]\} - \log_{10}\{{\rm f}\} \sim 0$, therefore, $f \sim 1$.

While this argument does constrain f for systems at the sharp transition between circularization and non-circularization, it does not rule out a dependence of f on period. In fact, the transition between circularized and non-circularized systems remains at $\log\{\Delta\ln[e]\} \sim 0$ if f scales as P^{1-x} with $1 \gtrsim x \gtrsim 0$ and has an appropriate normalization (see Fig. 2). This corresponds to $Q'_\star \propto P^x$. It is worth mentioning that the scaling used in Fig. 2 is one example among many that preserve the location of the transition. Different normalizations preserve the transition for different ranges of x. For example, $f = (P/200\,{\rm days})^{1-x}$, preserves the transition for $2 \gtrsim x \gtrsim 0$. The value $x = 2$ (for which $Q'_\star \propto P^{-1}$) has been urged by Goldreich and Nicholson (1977) in the limit $P \ll \pi\tau_{\rm conv}$; however, $P \gtrsim \pi\tau_{\rm conv}$ for most of the cases of interest to us.

Thus, by using Eq. (10), we are able to employ the tidal prescription of Zahn (1966) with the observational calibration of Verbunt and Phinney (1995). In Section 4, we show that employing such a formalism leads to values of $Q'_\star$ between $\sim 10^2$ and 10^3 for post-main sequence giants. These values are two to seven orders of magnitude lower than those typically invoked in the context of extra-solar giant planets (Goldreich and Soter 1966; Yoder and Peale 1981; Ogilvie

and Lin 2004, 2007; Jackson et al. 2009; Ibgui and Burrows 2009; Ibgui et al. 2010; Miller et al. 2009) and lead to strong tidal interactions. We pause to note that tidal theory is an active field of research (Goodman and Lackner 2009; Gu and Ogilvie 2009; Arras and Socrates 2009) Particularly relevant is a recent study that investigated a frequency dependence of Q' (Greenberg 2009). This work demonstrated that commonly used analytic approaches (which make analogy to a driven harmonic oscillator) are probably valid only for low eccentricities and inclinations. Theoretical and observational constraints on the tidal dissipation mechanism will help constrain the results of this work in the future.

For now, in light of the uncertainties in $Q'_\star$, and in f, we adopt the following form

$$Q'_\star = Q_0 \times \left(\frac{\Pi}{\Pi_0}\right)^x \tag{11}$$

where $\Pi \equiv P/\tau_{\rm dyn} = P\,(\rho G)^{1/2}$ is the orbital period divided by the dynamical time, Π_0 is a reference value, $\log_{10} Q_0$ is between 5 and 9. For Π_0, we use a 10 day orbital period divided by the dynamical time of the Sun, namely $\Pi_0 = (10\ {\rm days}) \times (\rho_\odot G)^{1/2}$. Note that even in the case where $f = 1$ and $x = 1$, Eq. (11) is not fully consistent with Eq. (10). For this paper, we focus on two representative values of x such that $Q'_\star \propto \Pi^0$ and $Q'_\star \propto \Pi^1$.

3 PRIMARY AND COMPANION MODELS

Our stellar evolution models are calculated using the "Evolve Zero-age Main Sequence (EZ) code" (Paxton 2004). For each initial stellar mass, we evolve the star from the ZAMS through the end of the AGB phase including a Reimers mass-loss prescription (Reimers 1975). In order to explore the influence of the rate of mass-loss on our calculations, we use a range of values of the Reimers η parameter: 0.7, 1, and 5. Each stellar model has a metallicity of $Z = 0.02$. In addition to the stellar radius and mass, we calculate the core mass and envelope binding energy as a function of time. Our stellar models (for $\eta = 1$) are presented in Fig. 3 while key parameters for all models are summarized in Table 1.

3.1 Companions

We consider three types of companions: planets ($M_c \lesssim 0.0026 M_\odot$; Zapolsky and Salpeter 1969), brown dwarfs ($0.0026 M_\odot \lesssim M_c \lesssim 0.077 M_\odot$; Burrows et al. 1993) and low-mass main sequence stars ($0.077 \lesssim M_c \lesssim 0.1 M_\odot$). We adopt the following approximation to the models of Burrows et al. (1993, 1997, 2001) for brown dwarf radii

$$R_2 = \left(0.117 - 0.054 \log_{10}{}^2 \left[\frac{M_c}{0.0026}\right] + 0.024 \log_{10}{}^3 \left[\frac{M_c}{0.0026}\right]\right) R_\odot\,, \tag{12}$$

and use a homologous power-law for low-mass stellar radii

$$R_2 = \left(\frac{M_c}{M_\odot}\right)^{0.92} R_\odot\,, \tag{13}$$

(Reyes-Ruiz and López 1999).

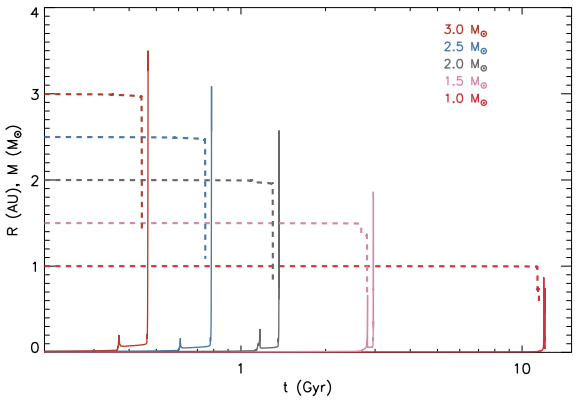

Figure 3. Mass (dotted line) and radius (solid line) profiles for a subset of our stellar models (i.e. those with $\eta = 1$). The mass profiles have been offset 5% in time so that the evolution is distinguishable on the plot.

We carry out our calculations for the following companions: a 0.001 $M_\odot$ (1 $M_{\rm J}$) planet, a 0.01 $M_\odot$ (10 $M_{\rm J}$) object that could be either a massive planet or a low-mass brown-dwarf (depending on formation scenario; hereafter referred to as a brown dwarf), and a 0.1 $M_\odot$ (100 $M_{\rm J}$) low-mass main sequence star.

4 TIDAL RESULTS

As the binary system evolves, mass-loss and tidal torques are in competition. Mass lost from the system acts to increase the semimajor axis while tidal torques decrease it. For each primary and companion, we compute the evolution of the orbit from the zero-age main sequence through the post-main sequence. If the companion is tidally captured (i.e. plunges into the primary star), it enters a common envelope with the primary and we halt the calculation of the orbital evolution. If the companion evades tidal engulfment, mass-loss continues and the orbit expands until the end of the evolutionary model.

We performed calculations for two tidal prescriptions: those corresponding to Eq. (2) and those corresponding to Eq. (10) when $f = 1$. With this approach, we can directly compare the tidal theories of Goldreich and Soter (1966) to those of Zahn (1966) when f is constant and equal to one (Verbunt and Phinney 1995).

For each stellar model, companion mass, and tidal theory, we calculate the maximum initial semimajor axis, $a_{\rm i,max}$, that is tidally engulfed. Eq. (2) is accurate to lowest order in eccentricity and valid for $e \ll 1$ (Goldreich and Soter 1966). For low e ($\lesssim$0.1), the effect of eccentricity is to modify the dominant tidal term by $\lesssim$10%. Thus, we assume circular orbits for the ensuing calculations. It should be noted that the formalism we employ only considers the quadrupole component of the tidal potential.

Although the Reimers prescription is an imperfect description of mass-loss, we investigate how different rates of mass-loss influence our results by using η values of 0.7, 1, and 5 (Reimers 1975). Our mass-loss prescription reproduces typical mass-loss rates during the RGB but underestimates

	$M_{\rm zams}$ ($M_\odot$)	$R_{\rm rgb}$[a] ($R_\odot$)	$M_{\rm rgb}$ (AU)	$R_{\rm agb}$ (AU)	$M_{\rm agb}$	$M_{\rm core,rgb}$[b c] ($M_\odot$)	$M_{\rm core,agb}$ ($M_\odot$)
	1.00	0.82	0.84	1.06	0.60	0.45	0.58
$\eta = 0.7$	2.00	0.27	1.98	2.81	0.90	0.38	0.81
	3.00	0.20	2.99	3.71	1.60	0.43	1.07
	1.00	0.87	0.73	0.75	0.56	0.46	0.56
	1.50	0.67	1.38	1.85	0.69	0.45	0.69
$\eta = 1$	2.00	0.27	1.97	2.57	0.80	0.39	0.81
	2.50	0.16	2.49	3.14	1.07	0.38	0.91
	3.00	0.20	2.98	3.50	1.40	0.44	0.99
	1.00[d]	0.41	0.38	–	–	0.37	–
$\eta = 5$	2.00	0.30	1.84	1.37	0.66	0.39	0.60
	3.00	0.20	2.94	2.50	0.81	0.43	0.75

[a] Maximum radius on the RGB/AGB.
[b] Calculated when the stellar radius is largest in the RGB and AGB phases.
[c] The core masses are defined by composition rather than degeneracy. Explicitly, it is the mass interior to the outermost hydrogen-free shell.
[d] The $\eta = 5$, 1 $M_\odot$ model does not achieve a sufficient core mass to undergo a helium flash.

Table 1. Stellar model data. Column quantities from left to right: zero-age main sequence mass, maximum radius on the RGB, stellar mass at the tip of the RGB, maximum radius on the AGB, stellar mass at the tip of the AGB, core mass for the corresponding $R_{\rm rgb}$, core mass for the corresponding $R_{\rm agb}$.

mass-loss rates on the AGB. As such, the results presented here serve as an approximate upper limit to the parameter space where tidal torques dominate over mass loss. Access to accurate stellar evolution models and realistic mass-loss prescriptions (motivated by observations during all phases of stellar evolution) will refine this work in the future (Schröder and Cuntz 2005, 2007).

4.1 When $f = 1$

The tidal theory of Zahn (1966) under the assumption that $f = 1$ has been employed to determine the effect of tidal torques on various aspects of post-MS evolution (Soker 1995, 1996; Villaver and Livio 2009; Carlberg et al. 2009; Bear and Soker 2009). This is accompanied by results that suggest strong tidal interactions for companions within $\sim(5-7)\times R_{\rm max}$, where $R_{\rm max}$ is the maximum radial extent of the star during either the RGB or AGB phases (Soker 1995, 1996; Debes and Sigurdsson 2002; Moe and De Marco 2006). Here, we make the same assumption and determine the maximum orbital separation that plunges into the primary star for various primary and companion masses.

Figure 4 shows $Q'_\star$ values at the time of tidal engulfment under the assumption that $f = 1$. Typically, values range from $10^{1.3} \lesssim Q'_\star \lesssim 10^{3.5}$, and, for a given progenitor mass, $Q'_\star$ values vary by less than a factor of $\sim$20, irrespective of the choice of η and companion mass. This is striking, as it implies that the assumption of $f = 1$ leads to tidal dissipation rates that are $\sim$2-7 orders of magnitude larger, in a dimensionless sense, than those acting on extra-solar giant planets. Typical $Q'_\star$ values for the transiting EGPs are typically taken to range from $10^5 - 10^8$ (Barnes et al. 2008; Jackson et al. 2009; Ibgui and Burrows 2009; Ibgui et al. 2010; Miller et al. 2009; Levrard et al. 2009).

With small $Q'_\star$ values, one would expect tidal engulfment to occur at large separations. Figure 5 shows the maximum semimajor axis that is tidally captured ($a_{\rm i,max}$) for a

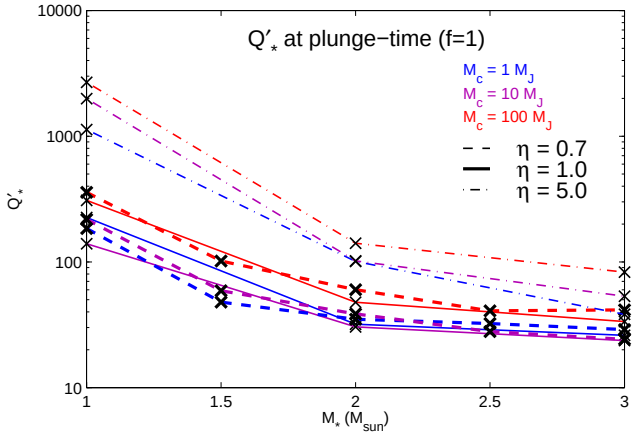

Figure 4. $Q'_\star$ values for post-main sequence binaries if $f = 1$. Note that choice of $f = 1$ yields $Q'_\star$ values 2 to 7 orders of magnitude lower than typical values used to explain the orbits and radii of transiting extra solar planets.

range of primary models and companion masses. The top panel presents $a_{\rm i,max}$ in units of AU for the case of $f = 1$, while the bottom panel shows the same results for the case of $Q'_\star = 10^5$ (see Table 1). Generally, the more massive stellar models extend to larger radii on the AGB and, therefore, can swallow companions that are farther away. Jupiter-mass companions within $\lesssim 2\times R_{\rm max}$ are captured while more massive companions can plunge at farther distances (10-Jupiter-mass companions are captured within $a \lesssim 2.5 \times R_{\rm max}$; 100-Jupiter-mass companions are captured within $a \lesssim 3\times R_{\rm max}$). It should be noted that the time of tidal engulfment roughly corresponds to the time at which the primary star is at its maximal radial extent. However, this is not exact as most binary systems are engulfed when the primary is still expanding, but near maximum radial extent.

If tides acting during the post-main sequence are char-

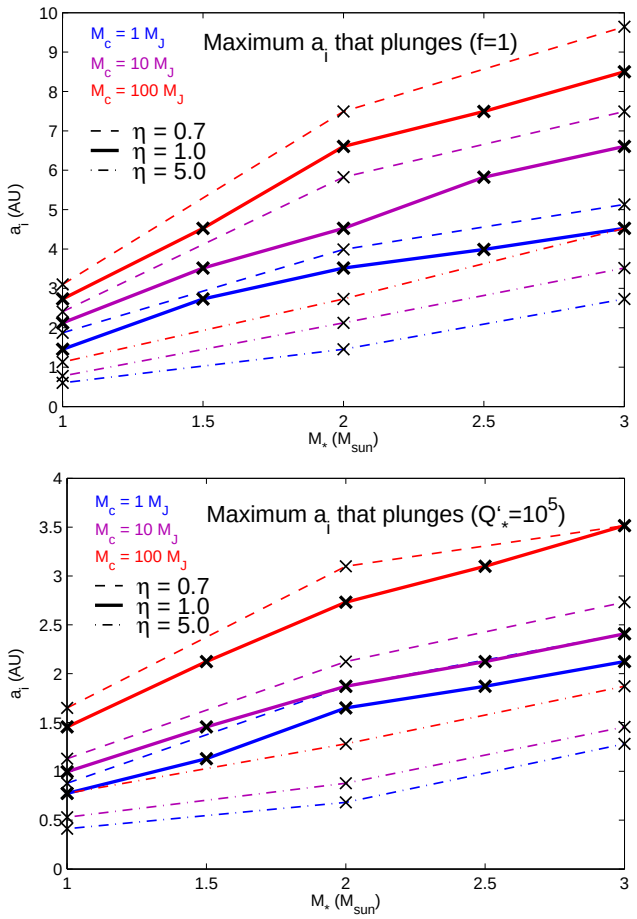

Figure 5. Maximum semimajor axis, $a_{\rm i,max}$ that is tidally engulfed under the assumption that $f = 1$ (top) and $Q'_\star = 10^5$ (bottom). Both figures present results for companions of mass $1M_{\rm J}$ (blue curves), $10M_{\rm J}$ (purple curves) and $100M_{\rm J}$ (red curves). Results for different mass-loss models are shown by $\eta = 0.7$ (dashed curves), $\eta = 1$ (solid curves), $\eta = 5$ (dot-dashed curves).

acterized by similar Q' values (in the Goldreich and Soter 1966 formalism) to those acting on EGPs during the main sequence (i.e., $Q'_\star \gtrsim 10^5$, $Q'_c \sim 10^6$), then results might be significantly different from those derived from the formalism of Zahn (1966) with $f = 1$ (in Fig. 5). To compare, in the next section we present cases in which $Q'_\star$ is constant and $Q'_\star \propto \Pi$.

4.2 $Q'_\star$ constant and $Q'_\star \propto \Pi$

The left columns of Fig. 6 show $a_{\rm i,max}$ as a function of primary mass for constant $Q'_\star$. The right columns present $a_{\rm i,max}$ for $Q'_\star = Q_0 \times (\Pi/\Pi_0)$. The evolutionary models in Fig. 6 were calculated with a Reimers mass-loss parameter of $\eta = 1$. The left plot is in units of AU while the right plot is in units of $R_{\rm max}$. As such, we can directly compare the results of a constant $Q'_\star$ to those of $f = 1$ shown in Fig. 5. Note that for $10^5 \leqslant Q'_\star \leqslant 10^9$ tidal torques are much weaker and result in smaller $a_{\rm i,max}$. In addition, the ratio $a_{\rm i,max}/R_{\rm max} \lesssim 1$ for most of the parameter space. For the same companion and stellar evolution model, $Q'_\star \propto \Pi$ produces larger $a_{\rm i,max}$ than the constant $Q'_\star$ case. Finally, for the EGPs, it may be that $x < 0$, consistent with the prediction that x should switch from $+1$ to -1 at $P \ll \tau_{\rm conv}$ (Goldreich and Nicholson 1977).

In order to estimate the effects of mass-loss, Fig. 7 shows $a_{\rm i,max}$ for $\eta = 0.7$ (left figure) and $\eta = 5$ (right figure). In general, less mass loss leads to tidal engulfment at slightly larger distances.

By coupling stellar evolution models with various tidal theories, we determined the maximum separation at which a companion might be tidally captured. Companions slightly exterior to $a_{\rm i,max}$ are never engulfed by the envelope of the primary but their orbital dynamics are still subject to the effects of mass loss and tidal torques. By continuing to follow the orbital evolution, we can predict the minimum final separation for each binary configuration. The minimum of this set is the minimum separation exterior to which one would expect to find planetary companions around white dwarfs.

In the following two sections, we determine the maximum separation at which a companion can survive CE evolution. Interior to this separation, we would expect to find companions to white dwarfs. Taken together, the minimum and maximum form a separation gap between which we expect an absence of planetary and brown dwarf companions around white dwarfs.

4.3 What About the Solar System?

For the solar system, tides and mass-loss compete and determine whether the inner planets plunge into the Sun or evade tidal engulfment (Rybicki and Denis 2001; Sackmann et al. 1993). Under the assumption $f = 1$, Venus plunges into the Sun for all of our 1 $M_\odot$ evolutionary models. Earth however, evades tidal engulfment with the orbit expanding for all of our evolutionary models, consistent with the results of Rasio et al. (1996). In addition, none of the planets beyond Earth are swallowed.

5 COMMON ENVELOPE EVOLUTION

Upon tidal engulfment, the companion enters a common envelope with the primary star (Paczynski 1976; Iben and Livio 1993; Nordhaus and Blackman 2006). The velocity difference between the orbital motion of the companion and the common envelope generates drag. The resulting loss of orbital energy leads to rapid in-spiral on week- to month-timescales (Nordhaus and Blackman 2006). The orbital energy released as the companion in-spirals can be used to overcome the binding energy of the envelope. If sufficient energy is released from the orbit during in-spiral, the companion can eject the envelope and survive the CE. This is expressed as the following:

$$E_{\rm bind} = -\alpha \Delta E_{\rm orb}, \tag{14}$$

where $E_{\rm bind}$ is the binding energy of the envelope, α is the fraction of orbital energy that goes toward ejecting the envelope and $\Delta E_{\rm orb}$ is the change in orbital energy of the companion.

The change in orbital energy of the companion is given as $E_{{\rm orb},R_\star} - E_{{\rm orb},a}$, where $E_{{\rm orb},R_\star}$ is the orbital energy at tidal engulfment ($a = R_\star$) and $E_{{\rm orb},a}$ is the orbital energy at

semimajor axis a inside the CE (i.e. $a < R_\star$). The orbital energy at tidal engulfment is given by the sum of gravitational and potential energies, namely:

$$E_{\rm orb,}{}_{R_\star} = -\frac{GM_\star\,[R_\star]\,M_c}{2R_\star} \quad (15)$$

where $M_\star[R_\star]$ is the total mass of the primary. The orbital energy at $a < R_\star$ is given by the kinetic energy (K_a) plus the gravitational potential energy (U_a):

$$\begin{aligned} E_{{\rm orb},a} &= K_a + U_a \quad (16)\\ &= \frac{GM_\star\,[a]\,M_c}{2a} - \frac{GM_\star\,[R_\star]\,M_c}{R_\star} - \int_a^{R_\star} \frac{GM_\star\,[r]\,M_c}{r^2} dr\,, \end{aligned}$$

where the integral term is the work against gravity required to move the companion from a to$R_\star$. The total change in orbital energy is then given as:

$$\begin{aligned} \Delta E_{\rm orb} &= E_{{\rm orb},a} - E_{{\rm orb},R_\star} \quad (17)\\ &= \frac{GM_\star[a]M_c}{2a} - \frac{GM_\star[R_\star]M_c}{2R_\star} - \int_a^{R_\star} \frac{GM_\star[r]M_c}{r^2} dr\,. \end{aligned}$$

The companion in-spirals until it is either tidally disrupted or supplies enough orbital energy such that $-\alpha\Delta E_{\rm orb} = E_{\rm bind}$ (Nordhaus and Blackman 2006). The binding energy of the stellar envelope is computed by summing the gravitational and thermal energies, at each evolutionary timestep. We require that the companion supplies enough orbital energy to overcome the binding energy of the entire envelope. If the companion only ejected the mass exterior to its orbit, the interior mass would expand to re-engulf the companion and restart in-spiral. Note that Eq. (17) depends on the stellar structure at the onset of tidal engulfment.

6 PERIOD GAPS FOR PLANETS AND BROWN DWARFS AROUND WHITE DWARFS

To calculate a minimum period gap expected for a given binary system, we assume $\alpha = 1$. This gives an upper bound on the orbital radius at which we would expect to find companions which have survived a common envelope phase (see Fig. 1). In §4, we determined the time at which a companion of mass M_c is engulfed by the giant star. Coupled with the structure of the star at the time of tidal engulfment, we can determine which semimajor axis a satisfies Eq. (14). If the companion avoids tidal disruption, then it has successfully ejected the envelope and survived the CE phase.

The tidal shredding radius can be estimated by balancing the differential gravitational force across the companion with its self gravity. This yields a tidal shredding radius given by $a_s \simeq R_c \sqrt[3]{2M/M_c}$ where R_c is the radius of the companion. For a $1M_{\rm J}$ companion around a proto-white dwarf core, $a_s \sim 7.4 \times 10^{10}$ cm. For a 10 $M_{\rm J}$ companion[1] $a_s \gtrsim 3 \times 10^{10}$ cm with the actual values dependent on the degenerate core mass during the CEP. If the companion unbinds the envelope exterior to a_s, then we say it has survived common envelope evolution. Note that the factor of $2M/M_c$ in the expression for a_s neglects the synchronous rotation of the companion and its finite Love number. Including these effects leads to a slightly larger tidal shredding radius, implying that slightly more massive companions are required to unbind the CE and avoid tidal disruption.

Since the stellar mass function is heavily weighted towards lower masses, we limit ourselves to a 1 $M_\odot$ progenitor. More massive primaries extend to larger radii (see Fig. 3) and swallow companions at farther distances, leading to wider period gaps. We consider two companions: a 1 $M_{\rm J}$ planet and a 10 $M_{\rm J}$ brown dwarf.

For each evolutionary model and binary configuration, we calculate the minimum and maximum bounds of the separation gap. Our results for $\eta = 0.7$, 1 and 5, $x = 0$ and 1 and $Q_0 = 10^6$ and $f = 1$ are summarized in Table 2. The maximum of $a_{\rm min}$ and minimum of $a_{\rm max}$ yield the minimum gap expected for a $M_\star = 1M_\odot$, $M_{\rm c} = 1M_{\rm J}$ system. Note that for pedagogical purposes we include the results for mass-loss only (no tides) in Table 2. However, when determining minimum period gaps, we only consider systems in which tides are acting. It should be stressed that even in the absence of tides, a minimum period gap exists. The functional dependence of tides on separation (Eq. 2) largely acts to change the location of the outer boundary of the gap. Depending on tidal prescription, this shifts the outer boundary of the by a factor of ∼2-3 at most (Table 2).

From Table 2, we see that there should be a paucity of Jupiter-mass companions with periods $\lesssim$270 days around white dwarfs. Additionally from Table 2, we see that there should be a paucity of 10 $M_{\rm J}$ companions with periods between 0.1 days (0.003 AU) and 380 days (0.75 AU). This is consistent with the tentative detection of a ∼2 $M_{\rm J}$ planet in a $\gtrsim$4 year ($\gtrsim$2.75 AU) orbit around the white dwarf GD 66 (Mullally et al. 2008, 2009). Future surveys for low-mass companions around white dwarfs will have the ability to confirm or refute our prediction of a gap. Several efforts are either recently completed or are currently underway (Farihi et al. 2006; Tremblay and Bergeron 2007; Hoard et al. 2007; Farihi et al. 2008; Farihi 2009). Once the samples are sufficiently large, observational identification of period gaps could help to constrain aspects of mass-loss and tidal theories.

For each $M_\star = 1M_\odot$ model, we can calculate the minimum mass companion able to unbind the envelope and survive a CE phase. This occurs when the binding energy of envelope is at a minimum. Note that, in multiple planet systems, several close companions may incur a CE phase. In conjunction, multiple lower-mass companions could potentially supply the same energy as a single larger mass object. Although we do not investigate such a scenario, multiple companions may successfully expel the envelope such that all or a subset survive. For the $\eta = 0.7$ model, the binding energy of the envelope is minimized when past the peak radius on the AGB. An 8.4 $M_{\rm J}$ mass companion is sufficient to unbind the envelope and survive a CE phase. For the $\eta = 1$ model, the envelope binding energy is minimized at the peak of the RGB. For this system, a 9.8 $M_{\rm J}$ companion is sufficient to survive a CE phase. The $\eta = 5$ model does not achieve a sufficient core mass to undergo a helium flash. As such, its maximal radial extent is less than the $\eta = 0.7$ and $\eta = 1$ models while the envelope binding energy is reduced. In this case, a ∼7.8 $M_{\rm J}$ mass companion is sufficient to survive a CE phase. For all of our models, most companions

[1] $M_{\rm J}$ is the mass of Jupiter.

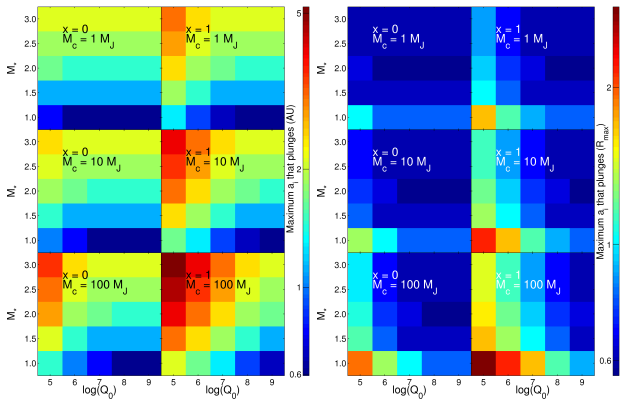

Figure 6. Maximum initial semimajor axis, $a_{\rm i,max}$, that enters a common envelope for 1, 10 and 100 $M_{\rm J}$ companions with 1, 1.5, 2, 2.5 and 3 $M_{\odot}$ primary stars. The left column in each figure presents results for $x = 0$ [$Q'_{\star} = Q_0$] while the right column presents results for $x = 1$ [$Q'_{\star} = Q_0 \times (\Pi/\Pi_0)$]. The evolutionary models of the primary star were computed with a Reimers mass-loss parameter of $\eta = 1$. The left figure is in units of AU while the right figure is in units of the maximum radius on the AGB (see Table 1).

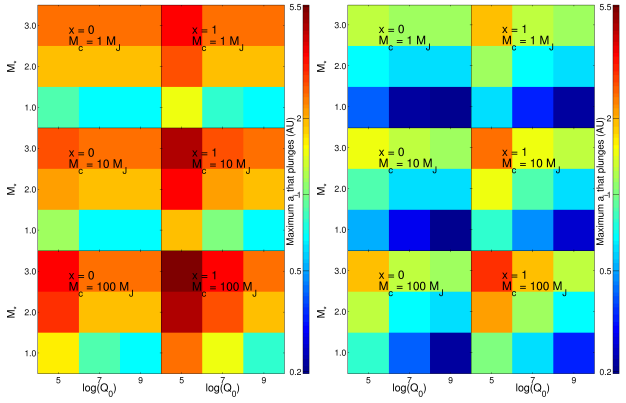

Figure 7. Maximum initial semimajor axis, a, that enters a common envelope for 1, 10 and 100 $M_{\rm J}$ companions with 1, 2 and 3 $M_{\odot}$ primary stars. The left column presents results for $x = 0$ [$Q'_{\star} = Q_0$] while the right presents results for $x = 1$ [$Q'_{\star} = Q_0 \times (\Pi/\Pi_0)$]. The color bar is in astronomical units. The evolutionary models of the primary star were computed with a Reimers mass-loss parameter of $\eta = 0.7$ (left figure) and $\eta = 5$ (right figure). In general, less mass-loss leads to tidal engulfment at a slightly larger semimajor axis.

more massive than $\sim$10 $M_{\rm J}$ will supply sufficient energy to unbind the envelope and survive the CEP at greater orbital separations.[2]

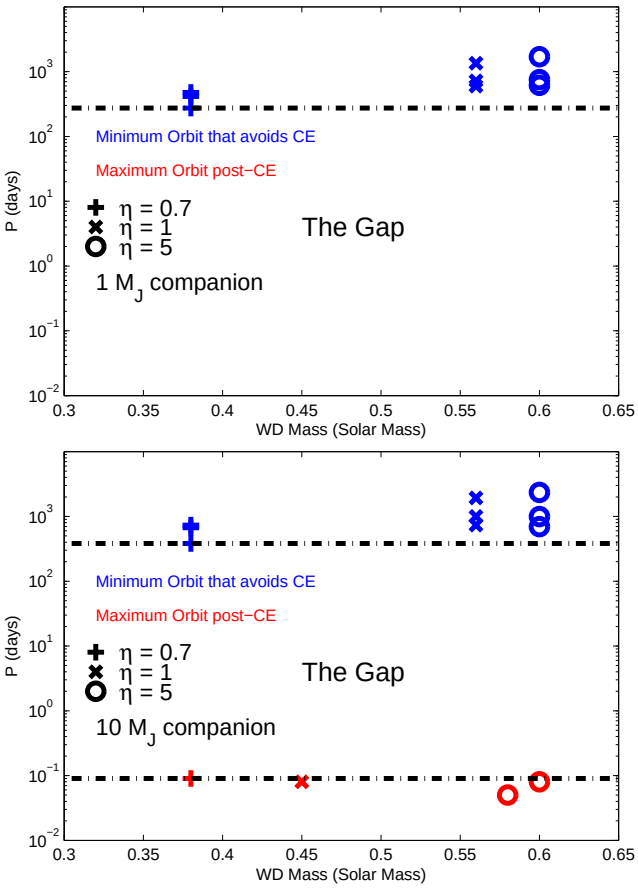

Figure 8. The predicted period gaps for a 1 $M_{\odot}$ progenitor with 1 $M_{\rm J}$ (top) and 10 $M_{\rm J}$ (bottom) companions. The symbols represent different Remiers η values for the various tidal prescriptions listed in Table 2. For the 1 $M_{\rm J}$ system, no companion survives CE evolution. Thus, we predict a paucity of 1 $M_{\rm J}$ companions with periods $\lesssim$270 days. For the 10 $M_{\odot}$ system, several companions survive CE evolution and are located in short-period orbits. The predicted period gap occurs between $\sim$0.1 and 380 days.

7 WD TRANSIT DETECTABILITY AND GALEX

If a massive planetary companion or a brown dwarf is engulfed and survives the common envelope phase, it could be left in a close, short-period orbit around the resultant WD. In such a scenario, if the orbit were oriented edge-on, it is conceivable that an entirely new regime of exoplanetary transiting observations would allow for detection of the companion. In contrast to the observations pioneered by Henry et al. (2000) and Charbonneau et al. (2000)[3], where transiting Jupiter-sized planets cause dips of $\sim$1% in the light curves of main sequence solar type stars, a massive Jupiter transiting a WD could cause a total eclipse (a 100% dip!). How likely are such detections? In this context, rather than the oft-quoted a priori probability of R_*/a that an exoplanet's orbit would be oriented so as to transit a main

[2] Note that even companions whose masses are several tens of Jupiter masses will still be within a few solar radii after surviving inspiral.

[3] See http://exoplanet.eu for an up-to-date census of the now more than 60 known transiting planets, and of all other known exoplanets.

		$M_\star$ ($M_\odot$)	M_c (M_J)	Q_0	x	$a_\mathrm{i,crit}$ (AU)	$M_\mathrm{core,1}$ ($M_\odot$)	$M_\mathrm{core,2}$ ($M_\odot$)	a_min [a] (AU)	a_max (AU)	P_min (days)	P_max (days)
	$\eta = 0.7$	1.0	1.0	–	–	1.90	–	0.60	–	2.36	–	1700
	$\eta = 1$	1.0	1.0	–	–	1.64	–	0.56	–	1.98	–	1350
	$\eta = 5$ [b]	1.0	1.0	–	–	0.64	–	0.38	–	0.79	–	414
$f = 1$	$\eta = 0.7$	1.0	10.0	–	–	2.53	–	0.60	–	2.93	–	2350
	$\eta = 1$	1.0	10.0	–	–	2.18	0.45	0.56	2.7×10^{-3}	2.51	0.08	1930
	$\eta = 5$ [b]	1.0	10.0	–	–	0.86	–	0.38	–	1.09	–	670
	$\eta = 0.7$	1.0	1.0	10^6	0	0.75	–	0.60	–	1.20	–	616
	$\eta = 0.7$	1.0	1.0	10^6	1	1.10	–	0.60	–	1.37	–	751
	$\eta = 1$	1.0	1.0	10^6	0	0.67	–	0.56	–	1.15	–	598
	$\eta = 1$	1.0	1.0	10^6	1	0.97	–	0.56	–	1.30	–	719
	$\eta = 5$ [b]	1.0	1.0	10^6	0	0.29	–	0.38	–	0.60	–	274
	$\eta = 5$ [b]	1.0	1.0	10^6	1	0.47	–	0.38	–	0.87	–	478
$Q'_\star \propto \Pi^x$	$\eta = 0.7$	1.0	10.0	10^6	0	0.93	0.60	0.60	2.7×10^{-3}	1.30	0.07	695
	$\eta = 0.7$	1.0	10.0	10^6	1	1.46	0.60	0.60	3.0×10^{-3}	1.65	0.08	993
	$\eta = 1$	1.0	10.0	10^6	0	0.79	–	0.56	–	1.32	–	736
	$\eta = 1$	1.0	10.0	10^6	1	1.30	–	0.56	–	1.62	–	1000
	$\eta = 5$ [b]	1.0	10.0	10^6	0	0.41	–	0.38	–	0.75	–	383
	$\eta = 5$ [b]	1.0	10.0	10^6	1	0.63	–	0.38	–	1.16	–	736
	$\eta = 0.7$	1.0	1.0	–	–	0.73	–	0.60	–	1.21	–	624
	$\eta = 1$	1.0	1.0	–	–	0.65	–	0.56	–	1.15	–	598
	$\eta = 5$ [b]	1.0	1.0	–	–	0.22	–	0.38	–	0.57	–	253
No tides	$\eta = 0.7$	1.0	10.0	–	–	0.73	–	0.60	–	1.21	–	624
	$\eta = 1$	1.0	10.0	–	–	0.65	0.45	0.56	2.7×10^{-3}	1.15	0.08	598
	$\eta = 5$ [b]	1.0	10.0	–	–	0.22	–	0.38	–	0.57	–	253
	$\eta = 0.7$	1.0	8.4 [c]	–	–	–	0.60	–	2.5×10^{-3}	–	0.06	–
	$\eta = 1$	1.0	9.8 [c]	–	–	–	0.45	–	2.2×10^{-3}	–	0.06	–
	$\eta = 5$	1.0	7.8 [c]	–	–	–	0.38	–	2.2×10^{-3}	–	0.06	–
$E_\mathrm{bind,min}$	$\eta = 0.7$	1.0	10.0	–	–	–	0.60	–	3.0×10^{-3}	–	0.08	–
	$\eta = 1$	1.0	10.0	–	–	–	0.45	–	2.7×10^{-3}	–	0.08	–
	$\eta = 5$	1.0	10.0	–	–	–	0.38	–	2.9×10^{-3}	–	0.09	–

[a] Companions which do not survive a common envelope phase are denoted by a $-$.
[b] The $\eta = 5$ model does not achieve a sufficient core mass to undergo a helium flash.
[c] The minimum mass companion required to unbind the envelope and survive a CEP.

Table 2. Period gaps for binary systems with different tidal formalisms ($Q'_\star \propto \Pi^x$; $f = 1$; no tides). The column quantities from left to right are Reimers mass-loss parameter η, $M_\star$ the mass of the primary star, M_c the mass of the companion, Q_0 [Eq. (11], x values such that $Q'_\star = Q_0(\Pi/\Pi_0)^x$ [Eq. 11], $a_\mathrm{i,crit}$, the critical initial radius below/above which the companion is/isn't engulfed (see Fig. 1), $M_\mathrm{core,1}$, the core mass for a_min, $M_\mathrm{core,2}$, the core mass for a_max, a_min the minimum separation (from CE evolution), a_max the maximum separation (from orbital evolution), P_min the minimum period (from CE evolution), P_max the maximum period (from orbital evolution). Companions that do not survive common envelope evolution are denoted by $-$. Note that the time of engulfment for the above cases does not necessarily coincide with the minimum binding energy of the envelope during its evolution. Therefore, we include results for companions entering the giant star at the time of minimum envelope binding energy ($E_\mathrm{bind,min}$). For graphical representations of this table see Fig. 8.

sequence star, the probability of a total eclipse in a system where $R_p > R_*$ is

$$p_\mathrm{orbit} \sim \frac{R_p}{a} \sim 0.1 \left(\frac{R_p/R_J}{a/R_\odot} \right) , \quad (18)$$

where R_J is Jupiter's radius, indicating that roughly one out of every ∼10 such post-CE systems might have an orbit that is oriented so that the companion eclipses the WD once per orbit. The duration of the eclipses will be of order

$$\delta_\mathrm{eclipse} \sim \frac{R_p}{2\pi a} \sim 2 \times 10^{-2} \left(\frac{R_p/R_J}{a/R_\odot} \right) \quad (19)$$

times the length of the year (P), or

$$\Delta t_\mathrm{eclipse} = \delta_\mathrm{eclipse} \times P \sim (4 \text{ min})(R_p/R_J) \sqrt{\frac{a/R_\odot}{M/(0.6 M_\odot)}} . \quad (20)$$

At any given time, the fraction of WDs being eclipsed by companions is of order

$$f_\mathrm{eclipse} \sim f_\mathrm{WD,p} \times \tilde{p}_\mathrm{orbit} \times \tilde{\delta}_\mathrm{eclipse} \quad (21)$$

$$\sim 2 \times 10^{-3} f_\mathrm{WD,p} \left(\frac{\tilde{R}_p/R_J}{\tilde{a}/R_\odot} \right)^2 ,$$

where $f_\mathrm{WD,p}$ is the fraction of WDs with short-period companions around them and $\tilde{p}_\mathrm{orbit}$, $\tilde{\delta}_\mathrm{eclipse}$, $\tilde{R}_p$, and $\tilde{a}$ are typical values of p_orbit, δ_eclipse, R_p, and a, respectively. The Galaxy Evolution Explorer (*GALEX*) is an ultraviolet space telescope capable of observing many hot WDs. Since *GALEX* time-stamps photons, it should be relatively easy to search the *GALEX* archive for transits. In order to detect an eclipsing system, a WD must be observed for a duration of at least $\Delta t_\mathrm{eclipse}$, or at two different epochs separated by at least $\Delta t_\mathrm{eclipse}$ such that it "winks out" and then reappears. Depending on the number of WDs that *GALEX* has observed (and on the duration of observations), a search of the *GALEX* archive might either detect some WD eclipsing binary systems – contingent on the distribution of radii and orbital semimajor axes of massive planets and brown dwarfs around WDs – or place constraints on the population of short-period companions to WDs.

7.1 Progenitors of Cataclysmic Variables

Via loss of orbital angular momentum, the short period systems that survive a CEP may be brought into Roche contact with the WD. Such systems may have been detected as cataclysmic variables (CV) but not recognized as post-planetary systems. If the donor is a massive planet with a rocky core, it may be possible for the core to survive the CV phase. This would result in a WD+rocky core short period binary.

8 CONCLUSIONS

By utilizing stellar evolution models from the ZAMS through the post-MS, we have followed the orbital dynamics of binary systems in which the companion is a 1 $M_{\rm J}$ planet, 10 $M_{\rm J}$ brown dwarf, or 100 $M_{\rm J}$ low-mass MS star. Our evolutionary models incorporate a range of mass-loss rates and stellar masses. Dynamically, the orbital evolution is subject to mass-loss (which acts to increase the separation) and tidal torques (which act to decrease the separation).

We employ two commonly used tidal prescriptions to investigate the differences during the post-MS. In particular, we find the following:

- The tidal theory of Goldreich (1963) under the assumption that $Q'_\star \sim 10^5 - 10^9$ leads to relatively weak tides, often capturing companions whose initial orbits are within $\sim 0.6 \times R_{\rm max}$, where $R_{\rm max}$ is the maximum stellar radius for an evolutionary model. Companions with initial orbits larger than $0.6R_{\rm max}$ but smaller than $R_{\rm max}$ can escape capture since their orbits expand due to mass loss of the primaries.
- The tidal theory of Zahn (1966), under the assumption that $f = 1$ (Verbunt and Phinney 1995), leads to comparatively strong tidal torques, often capturing companions within $\sim(2-3) \times R_{\rm max}$. Nevertheless, even this is less than the values of $\sim 5-7 \times R_{\rm max}$ that have been quoted in the literature (Soker 1996; Debes and Sigurdsson 2002; Moe and De Marco 2006).
- The ratio $a_{\rm i,max}/R_\star$, where $a_{\rm i,max}$ is the maximum radius that is tidally engulfed, is not constant.
- Future determination of the observational period gap for low-mass companions around WDs should help place constraints on the actual tidal theory acting in the post-MS.

For each tidal theory, we determined the maximum separation for which companions might be tidally engulfed (i.e. plunge into the primary star). These results serve as initial conditions for the onset of the common envelope phase for low-mass companions. Previous population synthesis predictions for post-AGB stars and PNe can be refined by incorporating the methods outlined in this paper.

For companions that incur a CE, under the assumption of maximum orbital energy deposition to the common envelope, we determined the maximum orbital radius at which a companion survives the interaction. By following the orbital evolution of the closest companion that evades tidal engulfment, we predict a period gap for each binary system.

For a binary system consisting of a 1 $M_\odot$ primary with a 1 $M_{\rm J}$ companion, we predict a paucity of Jupiter-mass companions with period below $\sim$270 days. For a 1 $M_\odot$ primary with a 10 $M_{\rm J}$ companion, the gap occurs between $\sim$0.1 and $\sim$380 days corresponding to $\sim$0.003-0.75 AU. Note that our estimated gaps are conservative and are obtained by finding the minimum gap that might be expected for a range of mass-loss rates and a range of assumptions about tidal dissipation. It is unlikely that the true gaps would be narrower than the ranges quoted above, but they easily could be wider. As our knowledge of stellar evolution and tidal dissipation improves, so will our estimates of the ranges for these gaps. Finally, we note that the results of surveys searching for low mass companions to white dwarfs might help to constrain theories of both stellar evolution and tides.

ACKNOWLEDGMENTS

We thank Brad Hansen, Frank Verbunt, Alex Wolszczan, Orsola De Marco, Eric Blackman, Jay Farihi, David Hogg, David Schiminovich, Claire Lackner, Fergal Mullally, Sarah Wellons, Rich Gott, and Kurtis Williams, for thoughtful discussions and comments.

Support for HPC storage and resources was provided by the TIGRESS High Performance Computing and Visualization Center at Princeton University. JG acknowledges partial support via NASA grant AST-0707373. AB and DS acknowledge support by NASA grant NNX07AG80G and under JPL/Spitzer Agreements 1328092, 1348668, and 1312647. This research was supported in part by the National Science Foundation under Grant No. PHY05-51164.

REFERENCES

Arras, P. and Socrates, A.: 2009, *ArXiv e-prints*
Balick, B. and Frank, A.: 2002, ARA&A **40**, 439
Barnes, R., Raymond, S. N., Jackson, B., and Greenberg, R.: 2008, *Astrobiology* **8**, 557
Bear, E. and Soker, N.: 2009, *ArXiv e-prints*
Bujarrabal, V., Castro-Carrizo, A., Alcolea, J., and Sánchez Contreras, C.: 2001, A&A **377**, 868
Burrows, A., Hubbard, W. B., Lunine, J. I., and Liebert, J.: 2001, *Reviews of Modern Physics* **73**, 719
Burrows, A., Hubbard, W. B., Saumon, D., and Lunine, J. I.: 1993, ApJ **406**, 158
Burrows, A., Marley, M., Hubbard, W. B., Lunine, J. I., Guillot, T., Saumon, D., Freedman, R., Sudarsky, D., and Sharp, C.: 1997, ApJ **491**, 856
Carlberg, J. K., Majewski, S. R., and Arras, P.: 2009, ApJ **700**, 832
Charbonneau, D., Brown, T. M., Latham, D. W., and Mayor, M.: 2000, ApJ **529**, L45
Chesneau, O., Clayton, G. C., Lykou, F., de Marco, O., Hummel, C. A., Kerber, F., Lagadec, E., Nordhaus, J., Zijlstra, A. A., and Evans, A.: 2009, A&A **493**, L17
de Marco, O.: 2009, PASP **121**, 316
De Marco, O., Hillwig, T. C., and Smith, A. J.: 2008, AJ **136**, 323
De Marco, O. and Moe, M.: 2005, in R. Szczerba, G. Stasińska, and S. K. Gorny (eds.), *Planetary Nebulae as Astronomical Tools*, Vol. 804 of *American Institute of Physics Conference Series*, pp 169–172
Debes, J. H. and Sigurdsson, S.: 2002, ApJ **572**, 556
Farihi, J.: 2009, MNRAS **398**, 2091

Farihi, J., Becklin, E. E., and Zuckerman, B.: 2008, ApJ **681**, 1470
Farihi, J., Hoard, D. W., and Wachter, S.: 2006, ApJ **646**, 480
Ferraz-Mello, S., Rodríguez, A., and Hussmann, H.: 2008, *Celestial Mechanics and Dynamical Astronomy* **101**, 171
Goldreich, P. and Nicholson, P. D.: 1977, *Icarus* **30**, 301
Goldreich, P. and Soter, S.: 1966, *Icarus* **5**, 375
Goldreich, R.: 1963, MNRAS **126**, 257
Goodman, J. and Lackner, C.: 2009, ApJ **696**, 2054
Gray, D. F.: 1989, ApJ **347**, 1021
Greenberg, R.: 2009, ApJ **698**, L42
Gu, P. and Ogilvie, G. I.: 2009, MNRAS **395**, 422
Henry, G. W., Marcy, G. W., Butler, R. P., and Vogt, S. S.: 2000, ApJ **529**, L41
Hoard, D. W., Wachter, S., Sturch, L. K., Widhalm, A. M., Weiler, K. P., Pretorius, M. L., Wellhouse, J. W., and Gibiansky, M.: 2007, AJ **134**, 26
Iben, Jr., I. and Livio, M.: 1993, PASP **105**, 1373
Ibgui, L. and Burrows, A.: 2009, ApJ **700**, 1921
Ibgui, L., Burrows, A., and Spiegel, D. S.: 2010, ApJ **713**, 751
Ibgui, L., Spiegel, D. S., and Burrows, A.: 2009, *ArXiv e-prints*
Jackson, B., Barnes, R., and Greenberg, R.: 2009, ApJ **698**, 1357
Jackson, B., Greenberg, R., and Barnes, R.: 2008, ApJ **678**, 1396
Jacoby, G. H.: 1980, ApJS **42**, 1
Kaula, W. M.: 1968, *An introduction to planetary physics - The terrestrial planets*
Kilic, M., Brown, W. R., and McLeod, B.: 2010, ApJ **708**, 411
Levrard, B., Winisdoerffer, C., and Chabrier, G.: 2009, ApJ **692**, L9
Livio, M. and Soker, N.: 1984, MNRAS **208**, 763
Massarotti, A., Latham, D. W., Stefanik, R. P., and Fogel, J.: 2008, AJ **135**, 209
Maxted, P. F. L., Napiwotzki, R., Dobbie, P. D., and Burleigh, M. R.: 2006, Nature **442**, 543
Miller, N., Fortney, J. J., and Jackson, B.: 2009, ApJ **702**, 1413
Miszalski, B., Acker, A., Moffat, A. F. J., Parker, Q. A., and Udalski, A.: 2009a, A&A **496**, 813
Miszalski, B., Acker, A., Parker, Q. A., and Moffat, A. F. J.: 2009b, *ArXiv e-prints*
Moe, M. and De Marco, O.: 2006, ApJ **650**, 916
Mullally, F., Reach, W. T., De Gennaro, S., and Burrows, A.: 2009, ApJ **694**, 327
Mullally, F., Winget, D. E., De Gennaro, S., Jeffery, E., Thompson, S. E., Chandler, D., and Kepler, S. O.: 2008, ApJ **676**, 573
Niedzielski, A., Goździewski, K., Wolszczan, A., Konacki, M., Nowak, G., and Zieliński, P.: 2009, ApJ **693**, 276
Nordhaus, J. and Blackman, E. G.: 2006, MNRAS **370**, 2004
Nordhaus, J., Blackman, E. G., and Frank, A.: 2007, MNRAS **376**, 599
Nordhaus, J., Busso, M., Wasserburg, G. J., Blackman, E. G., and Palmerini, S.: 2008a, ApJ **684**, L29
Nordhaus, J., Minchev, I., Sargent, B., Forrest, W., Blackman, E. G., de Marco, O., Kastner, J., Balick, B., and Frank, A.: 2008b, MNRAS **388**, 716
Ogilvie, G. I. and Lin, D. N. C.: 2004, ApJ **610**, 477
Ogilvie, G. I. and Lin, D. N. C.: 2007, ApJ **661**, 1180
Paczynski, B.: 1976, in P. Eggleton, S. Mitton, & J. Whelan (ed.), *Structure and Evolution of Close Binary Systems*, Vol. 73 of *IAU Symposium*, pp 75–+
Paxton, B.: 2004, PASP **116**, 699
Peimbert, M.: 1990, *Revista Mexicana de Astronomia y Astrofisica* **20**, 119
Qian, S., Liao, W., Zhu, L., Dai, Z., Liu, L., He, J., Zhao, E., and Li, L.: 2010, MNRAS **401**, L34
Rasio, F. A., Tout, C. A., Lubow, S. H., and Livio, M.: 1996, ApJ **470**, 1187
Reimers, D.: 1975, *Memoires of the Societe Royale des Sciences de Liege* **8**, 369
Reyes-Ruiz, M. and López, J. A.: 1999, ApJ **524**, 952
Rybicki, K. R. and Denis, C.: 2001, *Icarus* **151**, 130
Sabin, L., Zijlstra, A. A., and Greaves, J. S.: 2007, MNRAS **376**, 378
Sackmann, I., Boothroyd, A. I., and Kraemer, K. E.: 1993, ApJ **418**, 457
Sahai, R. and Trauger, J. T.: 1998, AJ **116**, 1357
Sato, B., Izumiura, H., Toyota, E., Kambe, E., Ikoma, M., Omiya, M., Masuda, S., Takeda, Y., Murata, D., Itoh, Y., Ando, H., Yoshida, M., Kokubo, E., and Ida, S.: 2008a, PASJ **60**, 539
Sato, B., Toyota, E., Omiya, M., Izumiura, H., Kambe, E., Masuda, S., Takeda, Y., Itoh, Y., Ando, H., Yoshida, M., Kokubo, E., and Ida, S.: 2008b, PASJ **60**, 1317
Schröder, K. and Cuntz, M.: 2005, ApJ **630**, L73
Schröder, K. and Cuntz, M.: 2007, A&A **465**, 593
Silvotti, R., Schuh, S., Janulis, R., Solheim, J., Bernabei, S., Østensen, R., Oswalt, T. D., Bruni, I., Gualandi, R., Bonanno, A., Vauclair, G., Reed, M., Chen, C., Leibowitz, E., Paparo, M., Baran, A., Charpinet, S., Dolez, N., Kawaler, S., Kurtz, D., Moskalik, P., Riddle, R., and Zola, S.: 2007, Nature **449**, 189
Soker, N.: 1995, MNRAS **274**, 147
Soker, N.: 1996, ApJ **460**, L53+
Spiegel, D. S., Goodman, J., Ibgui, L., Nordhaus, J., and Burrows, A.: 2010, *In prep.*
Tremblay, P. and Bergeron, P.: 2007, ApJ **657**, 1013
van Winckel, H.: 2003, ARA&A **41**, 391
Verbunt, F. and Phinney, E. S.: 1995, A&A **296**, 709
Villaver, E. and Livio, M.: 2007, ApJ **661**, 1192
Villaver, E. and Livio, M.: 2009, ApJ **705**, L81
Vlemmings, W. H. T., Diamond, P. J., and Imai, H.: 2006, Nature **440**, 58
Vlemmings, W. H. T. and van Langevelde, H. J.: 2008, A&A **488**, 619
Witt, A. N., Vijh, U. P., Hobbs, L. M., Aufdenberg, J. P., Thorburn, J. A., and York, D. G.: 2009, ApJ **693**, 1946
Yoder, C. F. and Peale, S. J.: 1981, *Icarus* **47**, 1
Zahn, J.: 1989, A&A **220**, 112
Zahn, J. P.: 1966, *Annales d'Astrophysique* **29**, 489
Zapolsky, H. S. and Salpeter, E. E.: 1969, ApJ **158**, 809